Passive Absorber to Reduce the Upper-Limbs Involuntary Tremor

S. GEBAI[a,b,c], G. CUMUNEL[a], M. HAMMOUD[b,c], G. FORET[a]

a. Université Paris-Est, Laboratoire NAVIER (UMR 8205), CNRS, Ecole des Ponts ParisTech, IFSTTAR, F-77455 Marne-la-Vallée, France
gwendal.cumunel@enpc.fr; sarah.gebai@enpc.fr; gilles.foret@enpc.fr
b. SDM Research Group, Department of Mechanical Engineering, International University of Beirut BIU, Beirut, Lebanon
c. School of Engineering, Lebanese International University LIU, Bekaa, Lebanon
mohamad.hammoud@liu.edu.lb; sarah.gebai@liu.edu.lb

Résumé :

Le post-traitement des signaux d'accélération mesurés au niveau de l'index d'un patient atteint de la maladie de Parkinson, ainsi que des signaux des muscles long extenseur radial (LRC) et fléchisseur radial (FRC) du carpe, générant le tremblement, sont présentés dans cette étude. La densité spectrale de puissance (DSP) de ces signaux est utilisée pour obtenir des informations sur les amplitudes et les fréquences du tremblement. Les signaux de mesure des muscles LRC et FRC présentent dans leur DSP des pics d'amplitude pour des fréquences de 6,6 Hz et 13,2 Hz, que sont également présents dans la DSP des signaux d'accélération. Les mesures des muscles sont ensuite utilisées en entrée d'un modèle dynamique dans le plan vertical d'un membre supérieur, où les mouvements angulaires de flexion/extension sont pris en compte au niveau des articulations. L'optimisation des paramètres d'amortisseurs à masse accordée passifs (AMA) est réalisée en utilisant ce modèle dynamique. La comparaison de différentes configurations d'AMA et certaines études paramétriques sont présentées et discutées.

Abstract :

Signal processing of the acceleration measured at the index finger of a Parkinson's disease (PD) affected patient, as well as of the signals of the Extensor Carpi Radialis longus (ECR) and Flexor Carpi Radialis (FCR) active muscles generating the tremor are processed in this study. The power spectral density (PSD) of these signals are used to obtain information about amplitudes and frequencies of the tremor. ECR and FCR signals measurements show critical peaks at 6.6 Hz and 13.2 Hz in their PSD, the same frequencies are present in the PSD of the acceleration signals. The muscles signals are scaled and used as input moment of a dynamical upper-limb model in the vertical plane, where flexion/extension angular motions are considered at the joints. The parameters optimization for the passive tuned-mass-dampers (TMD) is done using this dynamical model. A Comparison of different TMD configurations and some parametric studies are presented and discussed.

Keywords : Tremor measurement, signal processing, optimized absorber

1 Introduction

Studies lacks analysis on the biomechanics of tremor describing the back-and-forth movement of human upper limbs [1]. Researchers provide mathematical models of the human upper-limbs in the vertical [2] and horizontal [3] planes described as 2 degrees-of-freedom (DOF) linkage with flexion/extension motion at the shoulder and elbow joints. The movement of upper-limbs cannot be described by the dynamics of pure pendulums without taking care of the muscular torques producing the tremor [4].

Modeling of the active muscle's signal generating the tremor is the most critical element for the hand dynamics, since the system's response to be controlled will highly depends on this torque. It is suggested that the tremor behavior deviates from being periodic due to the second-order non-linear stochastic oscillator with an additive dynamic noise [5], and described by some researchers as harmonic oscillators with variable amplitude and/or frequency [6], diffusional processes [5], and Gaussian noise [7,8]. The research interest in modeling the hand's involuntary tremor and understanding its behavior is recently increasing [9,10], and can be used for designing a tremor control device [11,12]. Tremor activity can be recorded using the Electromyography (EMG), accelerometry, force measurements, or acquired gyroscopic measurements. To perform signal processing, it is preferable to have a recording device with at least 50 Hz sampling rate, since most biological tremors have a frequency of concern less than 25 Hz [13].

Active vibration controllers are usually used to reduce the hand motion at the undesired frequencies [11,14]. The active controllers require good knowledge about the characteristics of the tremor motion and the excitation source, in addition to a precise control force actuated by a large external power source. So, the use of passive tuned-mass-dampers (TMDs) to provide significant reduction in the motion along the undesired bandwidth can be a good replacement for the active control strategies.

In this study, the tremor's acceleration of a Parkinson's disease (PD) patient is measured in the three directions, and ideally complemented by the EMG measurements to document the rhythmic alternating activation in Extensor Carpi Radialis longus (ECR) and Flexor Carpi Radialis (FCR) muscles generating the tremor. Power spectral densities (PSD) of these signals are then calculated to identify the dominant peak frequency and its corresponding amplitude. We concentrate on the measurements within the frequency bandwidth 2–20 Hz since the tremor frequency range of interest is 3–12 Hz [15,16]. The human upper-limbs is modeled dynamically as a 3 DOF links system with flexion/extension motion at the joints, corresponding to the shoulder, elbow, and wrist joint. The measured ECR muscle's signal is scaled and used as an input moment. TMDs, located at the forearm or the palm of the modeled hand system, are optimized to reduce the involuntary tremor amplitude at the wrist joint. Different configurations of TMD are compared and some parametric studies are presented and discussed.

2 Signal Processing

Tremor is measured using a triaxial, accelerometer (PCB Piezotronics, Model 356A32). Department of Nervous System Diseases in 'Hôpital Pitié-Salpêtrière', Paris, are engaged in the determination of the hand tremor and muscles signals of a PD patient during typical neurological tests. The motion is measured with the accelerometer located at the index finger when the limbs are held horizontally against gravity, elbows are bent and hands facing each other (postural task). The measurements of the

hand and muscle's signals lasted for 60 s for the tremor data set with a sampling frequency of 5 kHz. The obtained data are downsampled with a ratio of 100 and filtered by a high pass filter having a cutoff frequency of 1.5 Hz. This helps reducing the undesired slow drifts and movement artifacts [1,17]. Then, the PSD is calculated for the downsampling frequency of 50 Hz using the Welch method with Hamming window of 256 points (5 s) and 80% overlap.
Tremor time series using the acceleration signals of the hand in addition to the EMG activity measurements of the muscles are provided by "Figure 1".

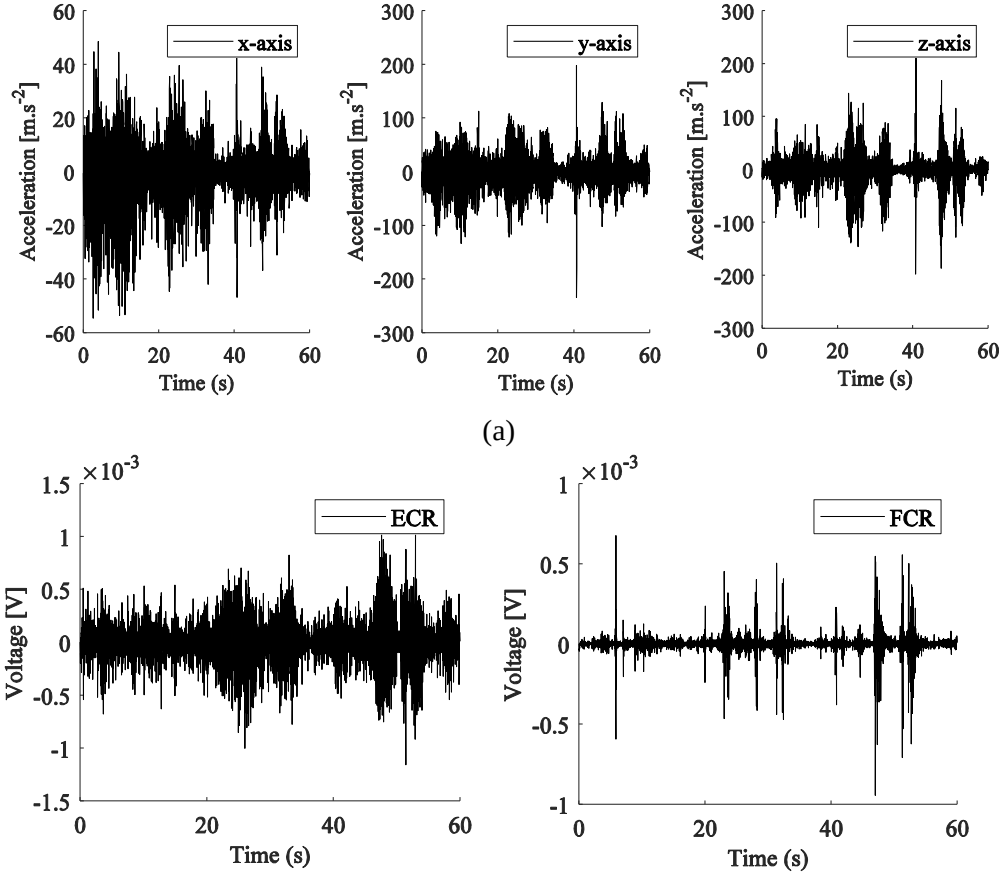

"Figure 1" (a) The measured acceleration signal at the finger in the x-, y-, and z-axis and (b) Electromyography recording of the ECR and FCR. ECR is the extensor carpi Radialis Longus, and FCR is the Flexor Carpi Radialis.

"Figure 1a" shows the acceleration of the palm when the accelerometer is placed at the index finger of the hand of the patient. The x-axis is the axial direction along the arm, directed from the front to back. The y-axis is the vertical, directed downward. The z-axis is the lateral axis directed from left to right. Tremor's acceleration in x-axis is less important than the tremor amplitude presented in the y and z-axis. The acceleration behavior in the three directions is very similar, but with different amplitudes. "Figure 1b" shows the measurements of the ECR and FCR muscles activity inducing the tremor, each muscle has its own behavior with different level of activation.
The PSD is used to acquire the amplitudes and frequencies of the measured signals. The PSD for the acceleration at the tip of the index finger in the three directions is presented in "Figure 2a", and compared with the ECR and FCR measurements in "Figure 2b". The hand's tremor acceleration in the x-, y-, and z-axis have peaks with different levels but at the same frequencies. The resonance

frequencies in muscle's PSD occurs at 6.6 Hz and 13.2 Hz which are exactly the same frequencies shown in "Figure 2a" for the hand's PSD in the three directions. This indicates that the muscles are driving the hand's tremor. In addition, the peak frequencies to be considered while controlling the hand tremor are the muscles peak frequencies and not the hand's fundamental frequency.

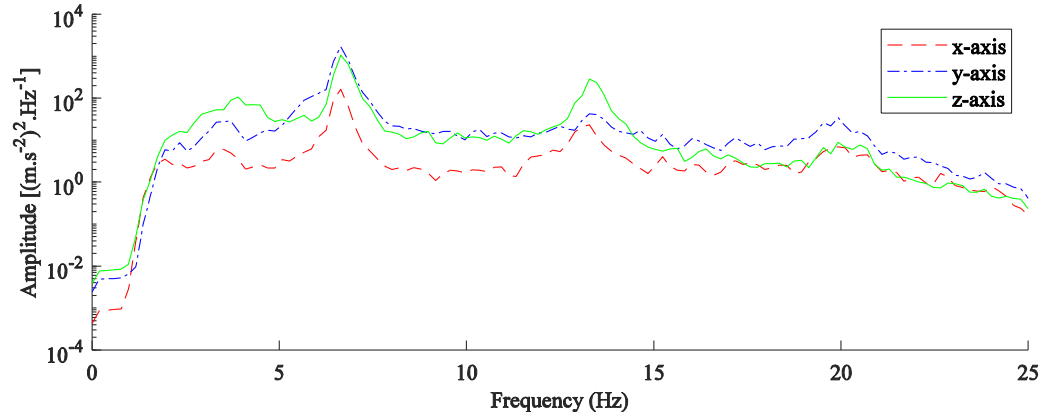

(a)

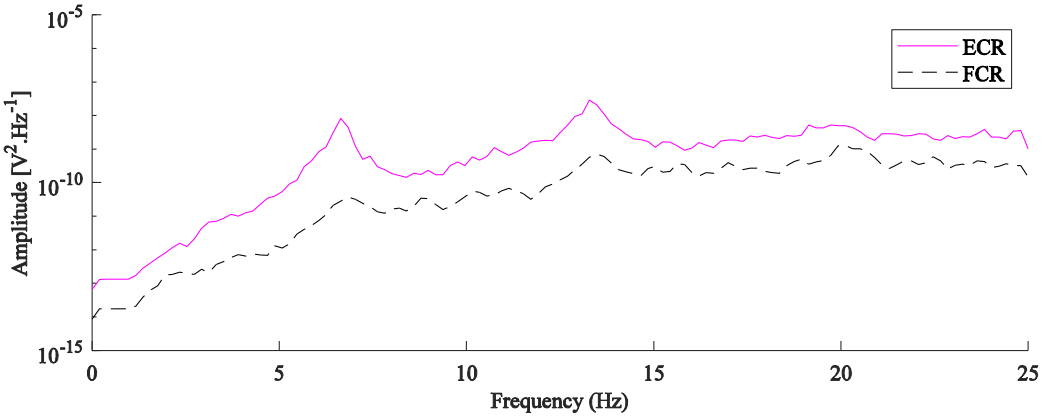

(b)

"Figure 2" Power spectral density of (a) the finger's acceleration in the x-, y-, and z-axis and (b) the ECR and FCR signals. ECR is the extensor carpi Radialis Longus, and FCR is the Flexor Carpi Radialis.

The PSD gives information about the dominant frequency of this patient, which occurs at 6.6 Hz within the bandwidth [6.2–7.0] Hz in x-, y-, and z-axis and represents the excitation frequency bandwidth of the muscle's signals. It is desired to reduce the amplitudes of the tremor all over this frequency range using passive TMDs.

The generated active torque of the muscles is unknown and no specific ready-to-use representative formula is found. So, the representation for the measured EMG signals can be helpful for the numerical study. Representing the muscle's torque as a sine function operating at the resonance frequency obtained from the measurements will lead to a PSD with a very narrow bandwidth just around this frequency. However, measurements of the muscle's signals in "Figure 2b" shows that the ECR and FCR have similar behavior with a broad excitation frequency bandwidth.

The half-power bandwidth method [18], can be then used to simply approximate the damping ratio of the dominant frequencies present in "Figure 2b". It leads to damping ratios of 2.8% and 1.7% for the ECR signal corresponding to the peaks at 6.6 Hz and 13.2 Hz, respectively. The muscle's signal shows

to have significant value of damping ratio, which could be used to formulate an analytical representation of the muscular torque.

3 Dynamic Hand Model

The upper limbs are modeled as three separated segments: the upper arm, forearm and the palm with masses concentrated at the centroid of each. The palm segment includes the index finger, and considered together as one segment. They are connected together by a 1 DOF shoulder, elbow, and wrist joints as shown in "Figure 3". A torsional spring and damper are modeled at each joint to reflect the effect of the passive muscles torque. The 3 DOF link-arm system is modeled in the vertical plane to permit the flexion/extension motion at the joints.

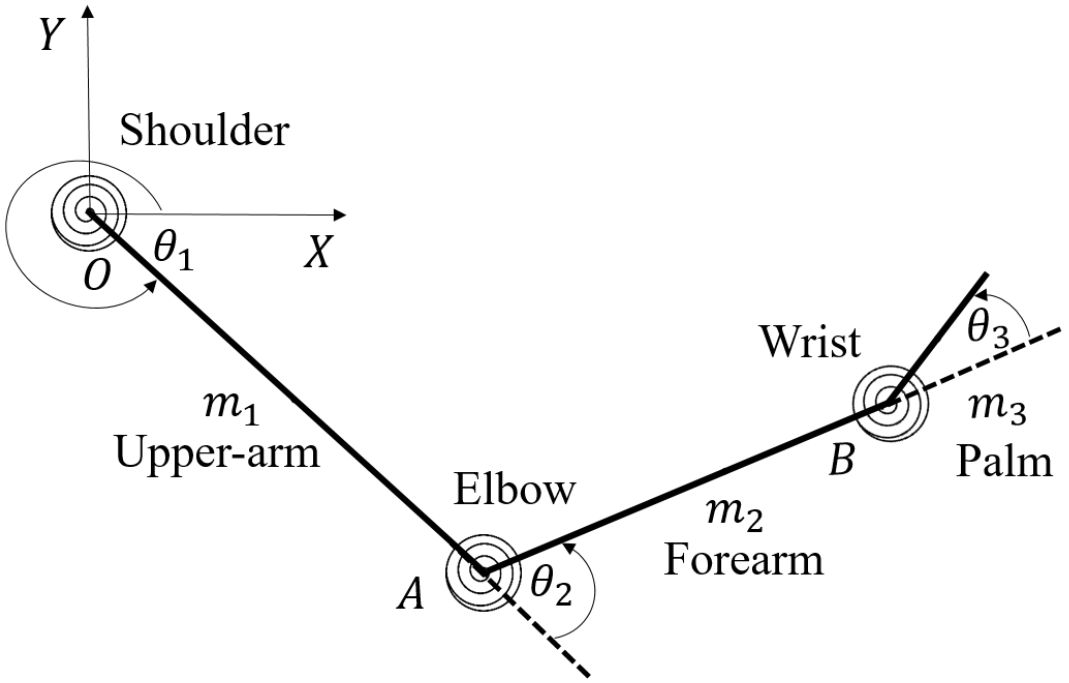

"Figure 3" Link-arm model of human's upper-limbs in the vertical plane. m_1, m_2, and m_3, and θ_1, θ_2, and θ_3 are the masses and the angular displacements of the upper-arm, forearm, and palm, respectively.

The muscles passive torque is considered as 90% due to elastic stiffness and 10% due to viscous stiffness as investigated in [19–21], where the stiffness range is between 0.1–10 $N.m.rad^{-1}$ [20]. This stiffness is used to be 10 $N.m.rad^{-1}$ to neglect the frictional effect within the joints. Then, the equation of the muscle's passive torque for the i^{th} DOF is:

$$\tau_{p_i} = \psi\left(0.9\,\theta_i + 0.1\,\dot{\theta}_i\right), \text{ where } \psi = 10\ N.m.rad^{-1} \tag{1}$$

where $\theta = \theta(t)$ and $\dot{\theta} = \dot{\theta}(t)$ are the angular displacement and velocity, respectively.

The governing equation of motion for the modeled system is derived using the Lagrange formulation of a non-conservative system as follows:

$$\frac{d}{dt}\left(\frac{\partial(T-U)}{\partial \dot{q}_i}\right) - \frac{\partial(T-U)}{\partial q_i} + \frac{\partial \Re}{\partial \dot{q}_i} = Q_i \text{ , such that } \Re_i = \frac{1}{2} c \dot{q}_i^2 \tag{2}$$

where T and U are the kinetic and potential energies. $q=\{\theta_1 \quad \theta_2 \quad \theta_3\}^T$ is the vector of the generalized flexion-extension angular displacements of the system. The indices *i*=1,2, and 3 refer to the shoulder, elbow and wrist, respectively. Q_i is the generalized conservative moments.

The kinetic energy (T) and total potential energy (U) of the system are:

$$T=\left[\frac{1}{2}I_1\dot{\theta}_1^2+\frac{1}{2}m_1v_1^2\right]+\left[\frac{1}{2}I_2\left(\dot{\theta}_1+\dot{\theta}_2\right)^2+\frac{1}{2}m_2v_2^2\right]+\left[\frac{1}{2}I_3\left(\dot{\theta}_1+\dot{\theta}_2+\dot{\theta}_3\right)^2+\frac{1}{2}m_3v_3^2\right] \tag{3}$$

$$U=m_1gr_1\sin\theta_1+m_2gr_2\sin\left(\theta_1+\theta_2\right)+m_2gl_1\sin\theta_1+m_3gr_3\sin\left(\theta_1+\theta_2+\theta_3\right)+m_3gl_2\sin\left(\theta_1+\theta_2\right) \tag{4}$$
$$+m_3gl_1\sin\theta_1+\frac{1}{2}k_1\theta_1^2+\frac{1}{2}k_2\theta_2^2+\frac{1}{2}k_3\theta_3^2$$

where k_i are the muscles stiffness, I_i is the moment of inertia of the arm, l_i is the length of the arm. v_i is the velocity at the location of the concentrated mass, g is the gravitational acceleration.

The Rayleigh dissipation function ($\Re$) due to the dampers at the joint is:

$$\Re=\frac{1}{2}c_1\dot{\theta}_1^2+\frac{1}{2}c_2\dot{\theta}_2^2+\frac{1}{2}c_3\dot{\theta}_3^2 \tag{5}$$

where, c_i is the muscles damping coefficient.

The obtained equation represents a dynamically coupled non-linear differential equation with high order and non-linear coefficients. The i^{th} DOF equation has the form:

$$\sum_j M_{ij}\ddot{\theta}_j=\sum_j P_{ij}\dot{\theta}_i\dot{\theta}_k+\sum_j N_{ij}\dot{\theta}_i^2+G_{i1}+\left(\tau_{a\,i}-\tau_{p_i}\right) \tag{6}$$

with $M=M(\theta,t)$ the mass moment of inertia matrix, $G=G(\theta,t)$ the vector of gravitational moments, $P=P(\theta,t)$ matrix is the coefficient of $\dot{\theta}_i\dot{\theta}_k$, $N=N(\theta,t)$ matrix is the coefficient of the $\dot{\theta}_i^2$. τ_a is the active torque of the muscles.

The equation of motion (6) is linearized around the static equilibrium position $\theta_0=\{\theta_{01} \quad \theta_{02} \quad \theta_{03}\}^T$, using Taylor's series, where the following linearized equation is obtained:

$$M\{\ddot{\theta}\}+C\{\dot{\theta}\}+(K+G_k)\{\theta\}=G_cV_{\theta_0}+G_k\theta_0+\tau_a, \tag{7}$$

$$\text{such that } V_{\theta_0}=\{\cos\theta_{01} \quad \cos(\theta_{01}+\theta_{02}) \quad \cos(\theta_{01}+\theta_{02}+\theta_{03})\}^T$$

where all the matrices have constant terms. K and C are the stiffness and damping matrices obtained using (1). G_k and G_c are obtained after the linearization of the non-linear gravitational terms. G_k acts as an additional stiffness for the system and also as a constant moment related to the presence of an initial static displacement θ_0. G_c acts as a constant applied moment which can always exist even in the stationary initial condition due to V_{θ_0}.

The response of the non-linear (6) and linearized (7) equations give the same responses in the time domain. In addition, the same responses are obtained in frequency domain for frequencies less than 16 Hz, which is greater than the frequency of interest for involuntary tremor analysis. This linearization permits to visualize the terms causing the homogenous response of the system which are always presented and needed for keeping the gravitational effect. The particular response is related to the active torque of the muscles. Thus, these two responses together reflect the response of the non-linear equation.

In order to obtain the response of the system in the frequency domain, Laplace transform (L) is done for the time-dependent differential equation (7). The frequency-dependent equation of motion becomes:

$$\{\Theta\}=\left(-\omega^2M+j\omega C+K+G_k\right)^{-1}.\left\{\left(j\omega M+C+G_k\right)\theta_0+G_cV_{\theta_0}+F\right\} \tag{8}$$

where ω is the angular frequency, $\Theta=\Theta(j\omega)=L\{\theta(t)\}$ and $F=F(j\omega)=L\{\tau_a(t)\}$

Equations (7) and (8) are used to determine the response of the modeled system, which can be used to optimize the TMD parameters.

4 Performance of Passive Absorber

The response for the frequency-dependent equation of motion (8) will be used to optimize the required suspension of the TMD (stiffness and damper), while specifying its proof mass, in order to reduce the maximum amplitude at the dominant frequency of the tremor. The TMD proof mass is expressed as a mass ratio percentage *(μ_a)* with respect to the upper-limbs total mass of 3.77 kg obtained using [22]. This study concentrates on the reduction of the flexion/extension angular motion at the palm joint.
The term 'F' in (8) is used to be the PSD of the scaled ECR active torque obtained from the EMG experimental measurement of "Figure 2". The implemented MATLAB program loads the patient's tremor data, solve the hand's equation of motion and then optimize the hand's response after the addition of the TMD(s). The passive TMD can operate on counter-acting the vibration of a specific undesired frequency. However, the operational bandwidth for the muscles of this patient is 0.8 Hz wide. The ability of several TMDs in covering the [6.2–7.0] Hz undesired bandwidth of this patient, around the 6.6 Hz dominant peak, will be studied.
"Figure 4" shows the response of the system before and after optimizing the TMDs located on the forearm. The position of the TMDs d_a along the forearm, measured from the segment's proximal joint, is 75% of its length, i.e. $d_a=0.75l_2$. "Figure 4a" compares the effect of adding 3, 4, and 5 optimized TMDs having the same total mass ratio μ_a=2%. The maximum reduction in tremor's amplitude caused by the addition of 5 TMDs, placed at the forearm, is about 37.6%. Increasing the number of TMDs on the forearm causes slight reduction the tremor's amplitudes as well as the operational bandwidth, so the 3 TMD case is chosen to test the effect of mass ratio.
"Figure 4b" shows the performance due to the addition of 3 TMDs to the system having 2%, 3%, and 4% mass ratio. The operational bandwidth of the 3 TMD covers the undesired range around the dominant frequency. "Figure 4b" shows that increasing the mass ratio causes significant reduction in the tremor amplitude. Since the system of interest represents the human's upper-limb, the focus will be on improving the performance of the light weight TMD, so the mass ratio μ_a=2% will be considered henceforward in the study.

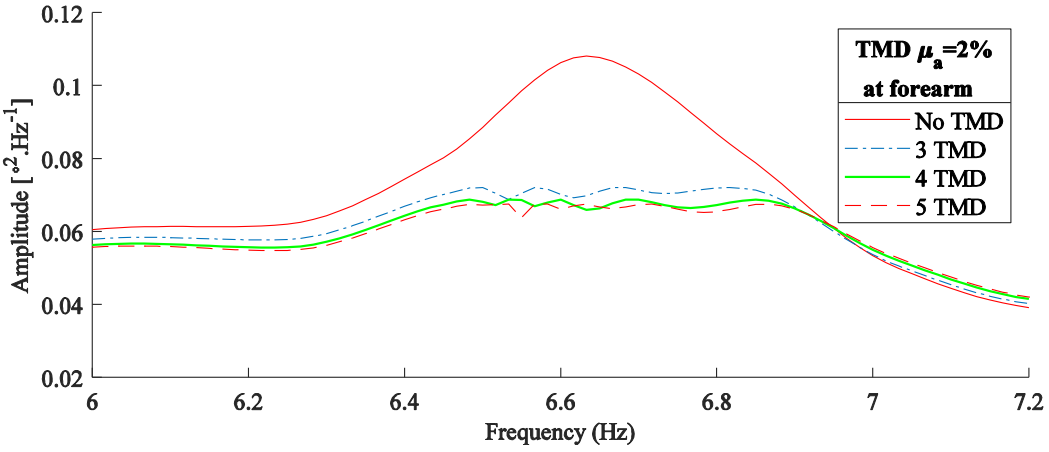

(a)

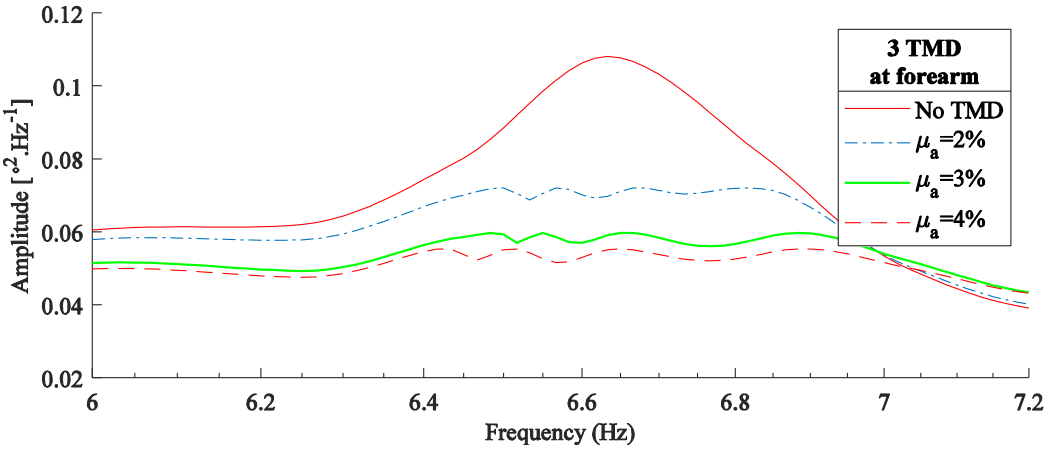

(b)

"Figure 4" Effect of optimizing the response of the modeled link-arm system for (a) 3, 4, and 5 TMDs with a total mass ratio of 2% and (b) 3 TMDs with 2%, 3% and 4% total mass ratio placed at the forearm. TMD is the tuned-mass-damper, and μ_a is the total mass ratio.

The performance of the optimized TMDs will now be tested when located along the palm segment of the hand for μ_a=2%. "Figure 5a" presents the effect of the optimized 3 TMDs for different position d_a measured from the segment's proximal joint. It shows that placing the TMDs away from the wrist joint causes more reduction in the tremor's amplitude. To avoid interference with the forearm segment and finger's joint, the middle tested distance will be chosen, i.e. $d_a=0.45l_2$. "Figure 5b" shows the addition of 3, 4 and 5 TMD having a 2% total mass ratio and placed $0.45l_2$ away from the wrist joint. The tested TMDs show reduction in the tremor amplitude which is higher than the one obtained upon the placement at the forearm. The 3, 4, and 5 TMDs caused 47.2%, 48.6% and 51.8% reduction at the maximum peaks, respectively.

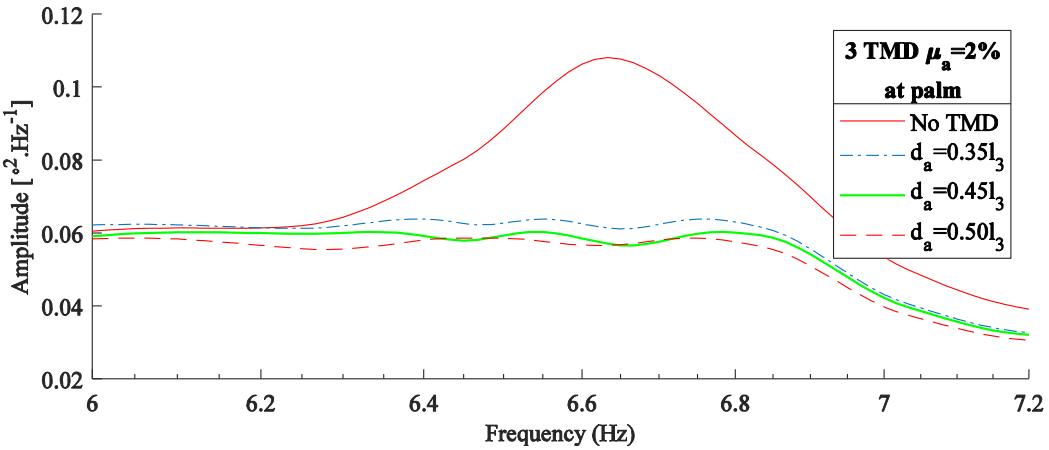

(a)

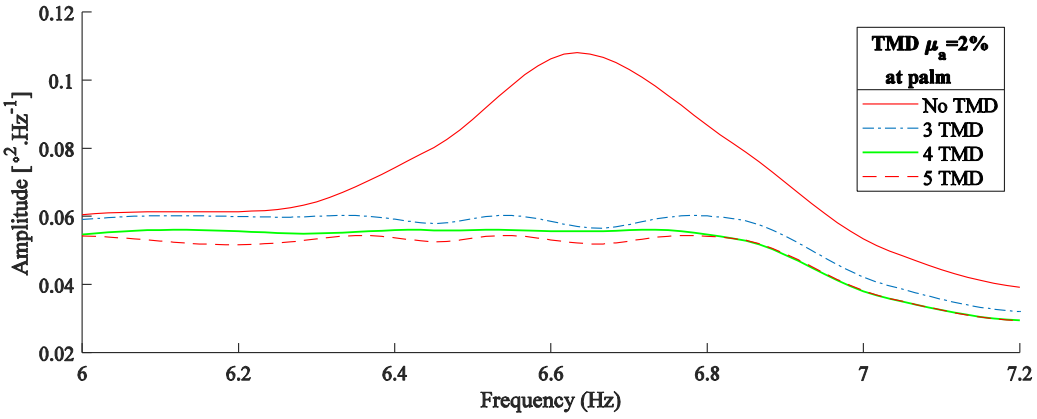

(b)

"Figure 5" Effect of optimizing the response of the modeled link-arm system for (a) TMDs placed at 35%, 45%, and 50% of the palm length away from the wrist joint and (b) 3, 4 and, 5 TMDs placed at the palm. TMD is the tuned-mass-damper, and μ_a is the total mass ratio.

5 Conclusion

Human hand tremor has been measured for a Parkinson's disease patient using an accelerometer located at the index finger and the EMG for the ECR and FCR active muscles generating the tremor. The PSD of the obtained measurements are used to identify the dominant frequencies of the patient's tremor, which is clinically used to quantify the severity of the involuntary tremor. The signal processing of the measured tremor raw data includes the signal's noise minimization, data filtering to preserve the desired frequency range for the study and measurements integration to provide additional data. Dynamic representation of the human upper-limb in the vertical plane is provided, derived using the Lagrange formulation, and solved numerically to determine the wrist joints response. The linearization of the equations of motion in time and frequency domains is used to simplify the complex equations, keeping high compatibility with the response of the non-linearized equations. This linearization helped to separate the system's parameters responsible for the homogeneous response and the others causing the particular responses of the upper-limb. Keeping the total response during the behavior analyses is essential to preserve the system's concept. Damping ratio calculation of the ECR signal is provided and suggested to be used for an analytical representation of the muscle's torque. The optimization of the passive multiple TMD is realized in order that the TMD can have a wide operational bandwidth which covers the excitation frequency bandwidth of the muscles. The TMD location at the forearm or palm segments is tested for different location along the segment, different mass ratios, and different numbers of TMDs. The optimization of the multiple TMD to reduce the tremor generated by the muscles provides acceptable tremor amplitude reduction. A 51% reduction of wrist joint's amplitude using a real muscle's torque signal was reached using 3 TMDs having a total mass ratio of 2% and located near the middle of the palm segment.

A similar study can be performed for several patients, for whom their tremor data have been measured for different hand positions and for several medical meetings. The study can give us more information about the acceleration ranges as well as the displacement amplitude of the tremor. The dominant frequency of each patient can be collected and comparison of the dominant frequency changes with position can be done. A comparison with the measured involuntary tremor data of healthy people will also be done to specify the severity of the patient's tremor level.

Acknowledgements

The authors gratefully acknowledge the hard work of Dr. Emmanuelle Apartis, Elodie Hainque, and Emmanuel Flamand-Roze, and their clinical teams from the Department of Nervous System Diseases of 'Hôpital Pitié-Salpêtrière'in Paris, whom provided us the measured data for the Parkinson patient who participated in this study.

References

[1] M. Mario, G. Giuliana, L. Thomas, F. Dario, P. Lana, C. Silvia, D. Tommaso, B. Juan-Manuel, P. Jose-Luis, R. Eduardo, Bioinformatic Approaches Used in Modelling Human Tremor, *Current Bioinformatics* 4 (2009) 154-172

[2] M. Nazari, G. Rafiee, A.H. Jafari, S.M.R.H. Golpayegani, Supervisory chaos control of a two-link rigid robot arm using OGY method, in: Proceedings of the IEEE Conference on Cybernetics and Intelligent Systems, Chengdu, China, 2008, pp. 41-46

[3] S. M. Hashemi, M.F. Golnaraghi, A.E. Patla, Tuned vibration absorber for suppression of rest tremor in Parkinson's disease, *Medical and Biological Engineering and Computing* 43 (2004) 61-70

[4] K.M. Jackson, J.T. Joseph, S.J. Wyard, A mathematical model of arm swing during human locomotion, *Journal of Biomechanics* 11 (1978) 277-289

[5] J. Timmer, S. Häussler, M. Lauk, C.H. Lücking, Pathological tremors: Deterministic chaos or nonlinear stochastic oscillators?, *Chaos: An Interdisciplinary Journal of Nonlinear Science* 10 (2000) 278-288

[6] M. Gresty, D. Buckwell, Spectral analysis of tremor: understanding the results, *Journal of Neurology, Neurosurgery & Psychiatry* 53(1990) 976-981

[7] J.B. Gao, Analysis of amplitude and frequency variations of essential and Parkinsonian tremors, *Medical and Biological Engineering and Computing* 42(2004) 345-349

[8] D. Buckwell, M.A. Gresty, Analysis of tremor waveform, in: L.J. Findley, W.C. Koller, (eds.), Handbook of Tremor Disorders, Marcel Dekker, New York, USA, 1995, pp. 145-164

[9] E.O. Ivanova, P.A. Fedin, A.G. Brutyan, I.A. Ivanova-Smolenskaya, S.N. Illarioshkin, Analysis of tremor activity of antagonist muscles in essential tremor and Parkinson's diseases, *The Neurological Journal* 19 (2015) 11

[10] S. Lee, W. F. Asaad, S. R. Jones, Modeling mechanisms of tremor reduction for essential tremor using symmetric biphasic DBS, *BioRxiv* (2019) 1-35

[11] D. Huen, J. Liu, B. Lo, An integrated wearable robot for tremor suppression with context aware sensing, in: 2016 IEEE 13th International Conference on Wearable and Implantable Body Sensor Networks (BSN), San Francisco, California, 2016, pp. 312-317

[12] E. Buki, R. Katz, M. Zacksenhouse, I. Schlesinger, Vib-bracelet: a passive absorber for attenuating forearm tremor, *Medical & Biological Engineering & Computing* (2017) 1-8

[13] C.W. Hess, S.L. Pullman, Tremor: clinical phenomenology and assessment techniques, *Tremor and Other Hyperkinetic Movements* 2 (2012) 1-15

[14] J. Leblanc, Design proposal for a mechanical tremor suppression device, Master's Thesis, Tufts University, Medford, 2005

[15] S. Reich, Common disorders of movement: Tremor and Parkinson's disease, in: Principles of Ambulatory Medicine, 4th ed., Williams and Wilkins: Baltimore, Massachusetts, USA, 1995, pp. 1217-1229

[16] R. Edwards, A. Beuter, Indexes for identification of abnormal tremor using computer tremor evaluation systems, *IEEE Transactions on Biomedical Engineering* 46 (1999) 895-898

[17] B. Taheri, D. Case, E. Richer, Robust controller for tremor suppression at musculoskeletal level in human wrist, *IEEE Transactions on Neural Systems and Rehabilitation Engineering* 22 (2014) 379-388

[18] M.J. Casiano, Extracting Damping Ratio from Dynamic Data and Numerical Solutions, in: Marshal Space Flight Center: Huntsville, Alabama, USA, 2016

[19] V. Wright, R. J. Johns, Physical factors concerned with the stiffness of normal and diseased joints, *Bulletin of the Johns Hopkins Hospital* 106 (1960) 215-231

[20] K.M. Jackson, J.T. Joseph, S.J. Wyard, A mathematical model of arm swing during human locomotion, *Journal of Biomechanics* 11 (1978) 277-289

[21] M. L. Corradini, M. Gntilucci, T. Leo, G. Rizolatti, Motor control of voluntary arm movement, *Biological Cybernetics* 67 (1992) 347-360

[22] Harless, E., The static moments of human limbs, *Treatises of the Math-Phys Class of the Royal Academy of Science of Bavaria* 8 (1860) 69-96 257-294